



Spring 2024

Jefferson County Ecological Conservation
Quantifying the Effects of Hydrologic Restoration in the Camas National Wildlife
Refuge and Mud Lake Wildlife Management Area

DEVELOP Technical Report

March 28th, 2024

Cassidy Bromka (Project Lead)

Rosemary D'Andrea

Matthew Stewart

Kevin Jo

Advisor:

Keith Weber, Idaho State University (Science Advisor)

Fellows:

Jane Zugarek (California - JPL)

Michael Pazmino (California - JPL)

1. Abstract

Wetlands in the Camas National Wildlife Refuge and Mud Lake Wildlife Management Area, a rare landscape feature in the Intermountain West, are crucial for migratory birds along the Pacific Flyway, yet these wetlands have experienced a noticeable decline in extent and inundation over the last 40+ years. Partners at the U.S. Fish and Wildlife Service and Idaho Department of Fish and Game have ongoing restoration efforts that are yet to be quantified. To assist these partners, we used NASA Earth observations to quantify change in wetland extent and determine if the restoration projects met the intended impact. The QA_PIXEL band from Landsat 5 Thematic Mapper (TM) and Landsat 8 Operational Land Imager (OLI) was used to identify water. Landsat 8 OLI imagery was also used for classifying landcover in ArcGIS Pro for 2016 and 2020 and to forecast landcover in 2060 using TerrSet's Land Change Modeler. We also compared lidar data from 2011 and 2019 to detect changes in vegetation height, ground elevation, and surface water levels, and Sentinel-2 Multispectral Instrument (MSI) imagery to detect changes in vegetation health. Classification results indicated overall accuracies over 84% and Kappa indices above 0.80, well surpassing random classification performance. From 2016 to 2020 our classifications showed an 825 acre increase in wetland extent, and our forecasted 2060 model showed a 2795 acre decrease. Combining our partners' knowledge of the area with our analyses, we created a remote sensing workflow to enhance future monitoring and decision-making. This study demonstrated the feasibility of NASA Earth observations in quantifying wetlands, informing restoration projects, and supporting avian conservation.

Key Terms

Landsat 5 TM, Landsat 8 OLI, Sentinel-2 MSI, lidar, remote sensing, wetland classification, wetland restoration, TerrSet Land Change Modeler

2. Introduction

2.1 Background Information and Scientific Basis

Wetlands provide crucial habitat for both resident and migratory animals. These habitats support a diverse array of life, offering critical feeding, breeding, and nesting grounds for wetland-dependent groups such as birds, amphibians, fish, and insects. Beyond their importance for wildlife, wetlands perform essential ecosystem services such as carbon sequestration, water quality improvement, and flood and erosion mitigation which contribute to climate regulation and protects human communities (Ma et al., 2018). Despite their invaluable contributions, these ecosystems face persistent threats from anthropogenic activities such as urbanization, unsustainable water usage, pollution, and global warming (Banerjee et al., 2016).

On a local scale, minor fluctuations in precipitation, snowpack, temperature, and vegetation can profoundly influence wetland ecosystems by causing changes in surface and ground water levels. Wetlands are sensitive to environmental variations, and Idaho historical data reflects significant challenges in wetland conservation. Between 1780 and 1980, there was an estimated 56% decrease in wetland acreage in the state of Idaho (Dahl, 1990), causing concern and sparking an increase in restoration efforts by the agencies that manage Idaho's wetlands. Measuring the efficacy of wetland restoration is both time-consuming and costly, and barriers associated with collecting field data have prompted a shift towards utilizing remote sensing technology. Specifically, the temporal and spatial analysis capabilities of remotely sensed data make it useful for mapping wetlands, monitoring long-term changes, and quantifying the impacts of restoration work (Sharma & Anjaneyulu, 1993; Ozesmi & Bauer, 2002; Huang et al., 2014). Efficient monitoring, exemplified by Idaho's investment in restoration projects, is essential for the maintenance of surface and groundwater levels.

Modern remote sensing methods commonly use data acquired from Earth observing sensors. Previous studies have demonstrated the capabilities of the multispectral sensors aboard Landsat satellites to provide wetland studies with the ability to determine surface water extent (Ashok et al., 2021; Naik & Anuradha, 2018). Previous wetland mapping studies have also utilized data collected through light detection and ranging (lidar; Huang et al., 2014). Lidar uses reflected light to collect elevation data which is later classified as vegetation, ground, and water. Currently, lidar requires aircraft for collection which can increase the cost of

research endeavors. However, its capacity to deliver fine spatial resolution and accurate elevation data offers a significant advantage in the execution of ecological studies. Inundation detection and analysis, using lidar collected across a temporal scale, are important for gauging how effective wetland conservation efforts are performing (Huang et al., 2014). In turn, the results can help determine the direction and extent of future restoration efforts.

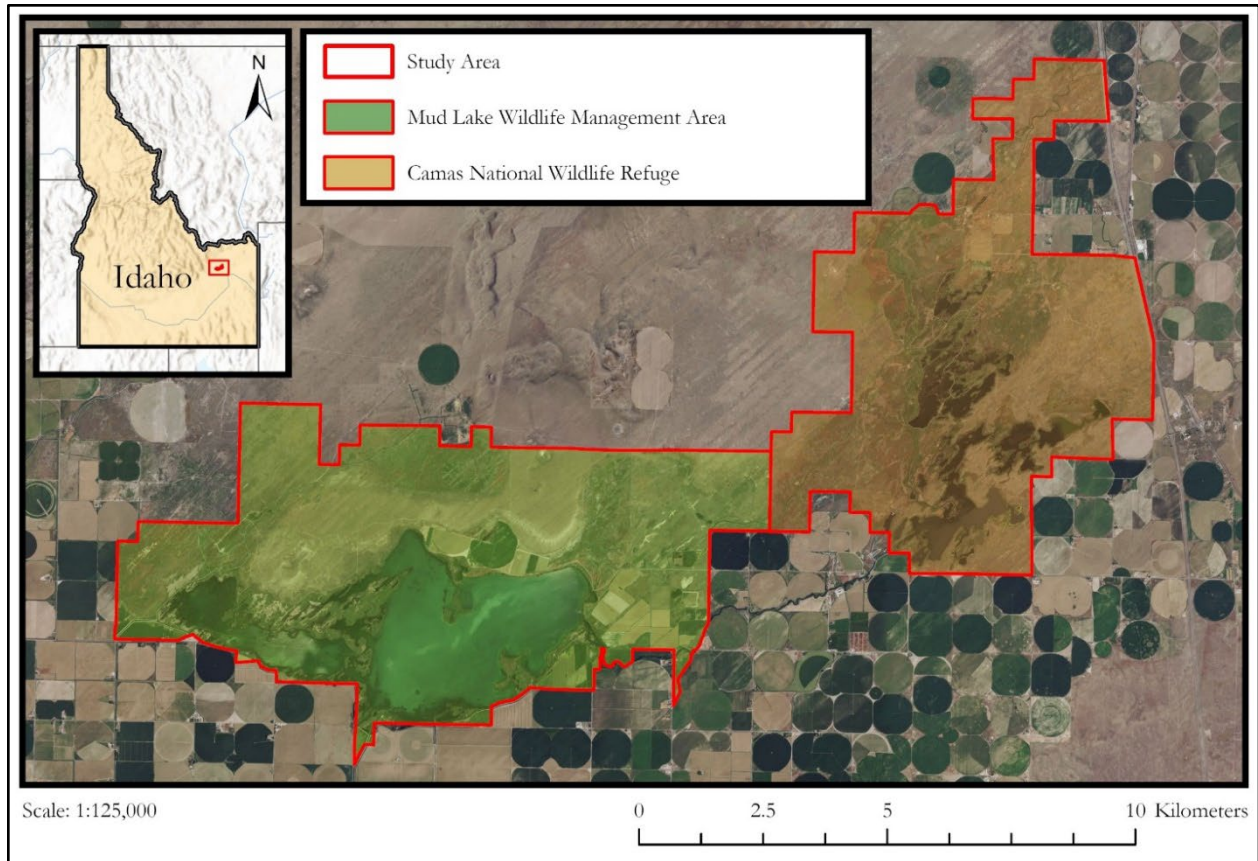


Figure 1. The study area encompassed Camas National Wildlife Refuge and Mud Lake Wildlife Management Area.

2.2 Study Area

The 24,620-acre study area encompassed Camas National Wildlife Refuge (NWR) and adjacent Mud Lake Wildlife Management Area (WMA) located in southeast Idaho (Figure 1). Within the Intermountain West, wetlands make up only 1% of surface area (Dahl, 1990). Because of the limited area of wetlands, both Mud Lake WMA and Camas NWR were established around 1940 with the mission of protecting crucial nesting and rest sites for waterfowl migrating along the Pacific Flyway (Camas National Wildlife Refuge, n.d.; Mud Lake WMA, 2023). Historically the landscape of what is now Mud Lake WMA was described as a shallow flat, where subsurface water was readily available and utilized by indigenous people. The advent of flood irrigation practices along the Egin Bench in the late 19th century led to an increase in subsurface water flow, contributing to the formation of Mud Lake. These irrigation practices also contributed to flourishing wetlands in Camas NWR in the 1980's.

Decreasing annual snowpack, stream incision of Camas Creek, excessive water uses by upstream farms, and changes in irrigation practices by nearby farms along the Egin Bench have contributed to a noticeable drop in the refuge and management area's water table. Since the 1990s, the wetlands in Camas NWR were no longer hydrated throughout the full brooding season of many waterfowl species (U.S. Fish and Wildlife Service, 2014). To combat the further decline of water inundation, wetland restoration efforts in this area have

become continuous, but have yet to be comprehensively evaluated. Some of the ongoing projects include conversion and creation of wet meadow habitat, enhancement of emergent wetlands around Mud Lake WMA, and rehydrating wetlands via groundwater pumping in Camas NWR.

2.3 Project Partners and Objectives

In partnership with the U.S. Fish and Wildlife Service (USFWS) and the Idaho Department of Fish and Game (IDFG), this project sought to quantify wetland extent and change. Due to current concerns over wetland extent and inundation, both USFWS and IDFG hold \$10 million and \$850,000 dollars respectively for wetland restoration projects, such as building wells to pump water to the surface, creating and improving canals to transport water to the wetland areas, and planting new cottonwood trees to replace dead trees. Thus, there was a need to devise a method to gauge the effectiveness of their restoration initiatives. To assist our partners with this management need, we investigated Earth observation data from 2011 to 2020 to examine how wetland extent, vegetation height, surface water, ground elevation, and Normalized Difference Vegetation Index (NDVI) changed over time. Additionally, we forecasted the wetlands' extent to 2060 using the trends found between 2016 and 2020. Analysis of our end products will help partners understand where their wetland restoration efforts are most effective and where to target for future restoration efforts. Overall, this project aimed to provide repeatable methods to produce data that can be used to guide future monitoring and decision-making.

3. Methodology

3.1 Data Acquisition

To determine the timeframe for our study, we compared the values for the Historical Palmer Drought Severity Index (PDSI; Table 3). We then selected years with values within the “normal” range so that excessive drought or flooding would not be a confounding factor in this study. We selected two time periods within each year: peak runoff (April–May) and the end of the growing season (August–September). This helped identify the variability in water level throughout the year. We decided to focus on 2016 and 2020 because there were similar values for drought indices throughout both the chosen months and years.

To acquire the necessary Earth observation data, we used the Google Earth Engine JavaScript API (GEE) platform. We used Landsat 5 Thematic Mapper (TM), and Landsat 8 Operational Land Imager (OLI) imagery to identify surface water extent throughout our study period (Table 1). For the Landsat data, we used Collection 2 Tier 1 Surface Reflectance because it is the highest quality data and was preprocessed & atmospherically corrected by the USGS. We focused on data from 2016 and 2020 because out of the years that had similar PDSI values, these years were the oldest (2016) and newest (2020) within the Landsat 8 collection. We also used Sentinel-2 Multispectral Instrument (MSI) to analyze vegetation health from 2016 to 2023 (Table 1). We acquired 2011 and 2019 lidar data from the Idaho Lidar Consortium (ILC) to analyze differences in topography and vegetation height between the collection times (Table 2). To help determine land cover classes, we referenced LandFire's (LF) Existing Vegetation Cover (EVC) and Existing Vegetation Type, as well as a Vegetation Dataset provided by our partners at the USFWS. To help ensure the accuracy of our 2060 model, we referenced the National Agriculture Imagery Program (NAIP) for Idaho from 2021 (Table 3).

Table 1.

List of Sensors and Data Products utilized for this project

Source	Resolution	Bands and Indices	Dates	GEE Image Collection ID
Landsat 5 TM	30 m	Red, Green, Blue, Near Infrared (NIR), Shortwave Infrared (SWIR), SWIR 2, QA_Pixel, MNDWI, NDVI	10/1 – 10/31 (2011)	LANDSAT/LT05/C02/T1_L2
Landsat 8 OLI	30 m	Red, Green, Blue, NIR, SWIR, SWIR 2, QA_Pixel, MNDWI, NDVI	3/1 – 11/30 (2016 – 2020)	LANDSAT/LC08/C02/T1_L2
Sentinel-2 MSI	10 m	NDVI	4/1 – 5/31 (2016 – 2023)	COPERNICUS/S2

Table 2.

List of lidar data utilized for this project

Source	Acquisition Method	Sensor	Resolution	Vertical Accuracy	Date Collected	Quality Level
US Fish & Wildlife Service (USFWS)	Idaho Lidar Consortium	Leica ALS50-II	0.4572 m	19.6 cm	10/19 – 10/20 (2011)	QL1
Federal Emergency Management Agency (FEMA)	Idaho Lidar Consortium	LMS-Q1560	1.3 m	9.8 cm	11/14 (2019)	QL1

Table 3.

Ancillary datasets utilized for this project

Source	Data Product	Dates	Acquisition Method
U.S. Fish and Wildlife Service	Camas National Wildlife Refuge Vegetation Inventory, Classification, and Mapping	Spring 2011 – Fall 2012	Given to us by Andrea Kristof of the USFWS
LANDFIRE (LF)	LandFire Existing Vegetation Cover (EVC), Existing Vegetation Type (EVT)	April 2016 – September 2020	Acquired, processed, and given to us by Keith Weber.
NOAA	Historical Palmer Drought Severity Index (PDSI)	April 2016 – September 2020	NOAA's Climate at a Glance Divisional Rankings website
U.S. Department of Agriculture (USDA)	National Agriculture Imagery Program (NAIP) of Idaho	June 2021	ArcGIS Online Portal

3.2 Data Processing

3.2.1 Classification Data

Within GEE, using Landsat 5 surface reflectance images over our study area for October 2011, and Landsat 8 for November 2019, we selected for QA identified water by masking out everything except water using bilinear bit for water for the QA_Pixel band, bit 7. We also filtered Landsat 8 surface reflectance images over our study area between April–May and August–September for 2016 and 2020. We then filtered out clouds using the QA band so that values would not be skewed when we reduced multiple images across months into one image. We also corrected a known Landsat 8 error that returns pixel values over water as negatives. We combined all the images across April–May and August–September for each year using median values. Furthermore, we exported the QA selected water maps and the blue, green, red, NIR, SWIR, and SWIR 2

bands of Landsat imagery as GeoTIFF files so each could be easily imported into ArcGIS Pro 3.2. We created layers of QA selected water to analyze the accuracy of it compared to water identified through Forest-based and Boosted classification, considering the former's potential ease of use for agencies with limited remote sensing expertise (Herndon et al., 2020).

Next, we used ArcGIS Pro for the calculation of the NDVI (Equation B1) and the Modified Normalized Difference Water Index (MNDWI; Equation B2) and for the creation of training and validation points for random forest classification. After visually inspecting and referencing EVC, EVT, and the vegetation classification dataset provided by the partners, we manually created a classification point layer identifying known areas of five land cover classes: water, wetland, developed, sagebrush steppe, and crops. The classification points ($n = 534$) were randomly divided in half using the subset tool in ArcGIS Pro to create separate training ($n = 267$) and validation points ($n = 267$). We created at least 60 points for each class so that after dividing them in half, each class would still have 30 points, which is the number frequently used as a statistically sufficient sample size.

3.2.2 Sentinel Data

Within GEE, we filtered Sentinel-2 surface reflectance images over our study area between April and May for the earliest year it was available, 2016, through the most recent year it was available, 2023. We then calculated NDVI (Equation B1) for each of those images, and then created one image for each year using the median values. These were then exported as GeoTIFF files and brought into ArcGIS Pro for visualization.

3.2.3 Lidar Data

We performed all lidar processing in ArcGIS Pro because of its three-dimensional data-handling capabilities. First, we collected preprocessed digital terrain models (DTMs) from the ILC for 2011 and 2019. These DTMs contain data for the elevation above sea level and are considered bare earth models. For the 2011 DTM, we mosaiced together each raster layer that intersected our study area and clipped them by our study area shapefile. The 2011 DTM was a hydro-flattened layer, so after clipping it, we applied the Fill function to fix pits, which are best described as irregularities in the data that often come from missing lidar data points. The 2019 DTM did not need to be mosaiced or "pit filled," but we did clip it to our study area. Lidar-derived DTMs provide fine spatial resolution (1-meter pixels), clipping them to the study area accelerated processing. Lastly, we used the 2019 DTM to create aspect and slope raster layers as predictor variables for our classification.

3.2.4 Lidar DSM Data

We also collected six preprocessed normalized digital surface model (DSM) raster layers that covered our study area for 2011. These DSMs showed the height of a surface relative to the ground rather than the elevation above sea level. We mosaiced these together and then clipped this layer to our study area. For 2019, we visually inspected the preprocessed DSM and found there to be errors, specifically negative values. So instead of using the preprocessed DSM we reclassified the raw lidar point cloud using the LASHeight tool. From there, we created a highest hit raster from the reclassified points.

3.3 Data Analysis

3.3.1 Classification

To run the Forest-based and Boosted Classification in ArcGIS Pro, for both 2016 and 2020, we input the training points ($n = 267$) for each year, the Landsat bands and indices, and lidar derived aspect and slope raster layers (Figure D5 and Figure D6). To analyze the output classification maps for each year, we used validation points ($n = 267$) to calculate confusion matrices. We also compared the two landcover classifications using TerrSet to visualize and quantify the changes between 2016 and 2020.

3.3.2 Forecasting Wetlands Extent

After classifying land cover for 2016 and 2020, we used TerrSet's Land Change Modeler to forecast the 2060 wetland extent. The model analyzes past land cover to predict future transitions. It used 2016 and 2020 data

to track landscape changes, focusing on elevation shifts and Idaho's decreasing precipitation to anticipate land cover evolution. We generated landscape projections for 2023 as this recent year serves as a benchmark to evaluate the model's short-term prediction validity. Any discrepancies found within this triennial forecast would cast doubts on the reliability of the model's long-term forecast to the year 2060. To bolster the precision of these forecasts, we refined the prediction transition matrix by assimilating both empirical observations and anticipated climatic evolution. Real-world discrepancies in the original probabilities necessitated a recalibrated computation. Given the absence of anticipated development or agricultural expansion within the study area, we adjusted the probability of land transitioning to developed or cropland categories to zero. A visual inspection of the predicted land cover for 2021 against the actual NAIP imagery captured in June of that year informed this recalibration. Table A1 shows the refined probabilistic parameters that yield the most precise predictions in alignment with the empirical data observed in the 2023 NAIP imagery. Incorporating these adjustments, the model recalibrated the predictions to align with the prevailing understanding that Idaho's climate is progressing toward increased aridity. This recalibration was pivotal in enhancing the model's predictive accuracy, ensuring that future forecasts of wetland extents are grounded in a comprehensive analysis of historical data and anticipated environmental changes.

3.3.3 Vegetation Health

To assess vegetation health and cover density, we created a time series in ArcGIS Pro of the NDVI images we gathered from Sentinel-2 (Figure D1). This allowed us to visually compare the NDVI values between each year to better understand what changes might have occurred regarding vegetation dying. After processing the full study area extent, we investigated regions of the study area map where known vegetation decline or planting occurred.

3.3.4 Lidar

We analyzed elevation and surface water level changes by comparing the hydro-flattened DTMs from 2011 and 2019. The DTM from 2011 was subtracted from the DTM from 2019, with the QA water masked out, to produce an elevation change map. We also reversed this process, so the DTMs covered only the water areas to produce a water level change map. To analyze the change maps, we observed the distribution of the changes for both elevation and water level. The elevation change values ranged from -3.93 m to 4.85 m, which we classified into six categories: less than 0 (encompassing all negative values), 0 to 0.97, 0.97 to 1.94, 1.94 to 2.91, 2.91 to 3.88, and 3.88 to 4.85. Recognizing the inherent uncertainties dictated in the lidar datasets, a combined root mean squared error (Equation B3) was calculated to be 0.0963 m. We also analyzed changes in vegetation height by subtracting the 2011 preprocessed DSM from the 2019 DSM we created.

4. Results & Discussion

4.1 Analysis of Results

4.1.1 Classification

After running the land cover classifications for 2016 and 2020 with the training points (Figure D5, Figure D6), we compared them to the validation points to create confusion matrices (Table A2, Table A3). The classification for 2016 reported 86.5% overall accuracy, with the most accurate class being water with 90.9% producer's accuracy, and 100% user's accuracy. The least accurate classes were developed and sagebrush. User accuracies were 74.1% and 85.7% respectively, and producer's accuracies were 78.4% and 91.4% respectively. The Kappa index of agreement (KIA) value was 0.83, which suggests our classification performed 80% better than a purely random classification. The classification for 2020 resulted in 84.27% overall accuracy, with the most accurate class again being water with 95.5% producer's accuracy and 93.3% user's accuracy. The least accurate classes were again developed and sagebrush. Users' accuracies were 85.2% and 75.0% respectively, and the producer's accuracies were 75.4% and 87.50% respectively. KIA was 0.80, which meant that although this classification was significantly more accurate than a random classification, it was slightly less accurate than the 2016 classification.

We then compared the two classifications to each other to understand the differences between them, or the changes that our classifications identified that had happened to the landscape. From 2016 to 2020 the water

class overall increased by 8.28%, 825 acres, and the wetlands class overall increased by 4.37%, 164 acres. Visually, the areas that gained wetlands were the northern and eastern parts of Camas NWR and the western part of Mud Lake WMA. The areas that lost some wetlands were the western part of Camas NWR and the northeastern and northwestern parts of Mud Lake WMA.

Although both classifications were statistically accurate, they showed discrepancies between the generated classifications and our partners' observations, i.e., both classifications greatly overestimated wetlands. This was most likely due to our creation and selection of classification points based on visual references without any in situ data to confirm whether the points we created for wetlands were wetlands on the ground. If we selected points that were not wetlands on the ground, this could have caused the classification's decision tree to interpret wetlands to encompass more area based on a wider range of spectral signatures from the training points.

4.1.2 Wetland Extent 2060 Model

After running our forecasted model with predicted land cover for 2060 (Figure D7), we compared it to our 2020 classification to understand what changes the model predicts to happen. From 2020 to 2060 it was predicted there would be a 38.96% decrease in wetlands, or 2795.65 acres, and a 27.98%, or 1458.93 acres, increase in open water (Figure C3). Visually, the areas gaining the most water were the southwestern part of Camas NWR and the northwestern part of Mud Lake WMA. Again, visually, the areas gaining some wetlands were the western part of Camas NWR and the western part of Mud Lake WMA, and the areas that were lost the most were the northern and eastern parts of Camas NWR and the northwestern part of Mud Lake WMA. Due to an error in the training set from 2016 to 2020, the prediction calculations amplified this issue. Although calibration efforts aimed to minimize this error, the underestimation of open water areas and overestimation of wetlands continued to affect future predictions.

4.1.3 Sentinel-2 NDVI Assessment

The NDVI assessment from 2016 to 2023 had an overall minimum value of -0.34 and maximum value of 0.82 . Values close to one represent healthy vegetation, values closer to zero show unhealthy vegetation such as dry grass and stressed herbaceous plants, and values close to zero are non-vegetation features such as water. Our NDVI time series (Figure D1) showed that 2016 had more stressed vegetation and less surface water than the following years. Most of the visible change between years was the red regions in Camas NWR, which indicates surface water extent. This shows us that water and vegetation health varied greatly each year, however, each year represents only the median NDVI for all of April to May, so this is not meant to be a comprehensive analysis of water extent and vegetation health change. Factors such as timing of snow melt, annual snowpack, drought, and timing of ground water pumping into the study area could all affect the observed NDVI.

4.1.4 Lidar Elevation and Water Level Changes

After comparing lidar between 2011 and 2019, we discovered a discrepancy in the 2019 DTM hydro-flattened product. This variance was initially noticed through visual differences in the elevation and water level change maps during hillshade creation, suggesting significant deviation in the 2019 elevations compared to 2011 (Figure D2). Further investigation revealed the breaklines used for the DTM, as discussed in the ILC lidar processing report, do not include the Mud Lake WMA and Camas NWR project area. The southwest regions of Camas NWR were particularly affected, where the reported elevations were implausibly high, suggesting non-existent drastic landscape changes. The areas' accuracy is critical due to concerns about sediment buildup at the inlets, which inhibits accurate assessment. This sediment could reduce water delivery, decreasing water levels and wetland extent.

The lack of breaklines in the Mud Lake WMA and Camas NWR project area indicates a fundamental flaw in the 2019 DTM product when assessing centimeter-level elevation differences. This analysis requires a reclassification of the breaklines for accurate assessments between 2011 and 2019 elevation and water levels. Accordingly, any conclusions drawn regarding elevation and water level changes between 2011 and 2019,

based on the available 2019 lidar DTM product data for this study area from the ILC, are unreliable. Corrective actions, including generating breaklines for this study area and a thorough reanalysis of the elevation comparison, is imperative to ensure the integrity of the study's findings, which was not feasible within the time constraints.

4.1.5 Lidar Vegetation Height Changes

Most of the study area experienced very little change vegetation heights, with a mean height change of +1.6 cm. The riparian area in the southwest region of Mud Lake WMA showed some new vegetation growth along the edges, with height values ranging from five to twelve meters of growth (Figure D3). Riparian areas in Camas NWR and Mud Lake WMA, and the planted shelter belt in Camas NWR (Figure D4), showed a large decrease in height of cottonwood trees (-29.5 meters), and an intermediate decrease in vegetation height of up to five meters for the willow trees on the northwest edge of Mud Lake. Upon referencing NAIP imagery for 2019, and field validation, we realized many of the areas showing drastic negative change over tall vegetation were incorrect, as vegetation in those areas was still present. Looking at the reclassified 2019 lidar point data and the resulting highest hit raster layer, it appeared that many of the canopy areas did not have canopy height values as expected but instead had values similar to the ground. We determined that the lidar point cloud data for 2019 did not support classification of many of the tall and medium height vegetation points, leaving them as unclassified. As a result, only bare ground returns were available for these areas. When we created the difference in canopy height raster between the two years, this classification omission resulted in some areas of very large change. This classification error also explains the maximum height increase of 29.77 meters as it is highly unlikely that a tree could grow this much in just eight years.

4.2 Feasibility for Partner Use

Although we found many of our methods feasible for partner use, the greatest limitations that we encountered were the errors in the preprocessed lidar data from 2019, the manual creation of training points for classification, and that the 2060 classification is only a prediction based on the land cover layers developed for this study and is not a certainty of what the future will look like. We found that the preprocessed DTM lidar data from 2019 contains variations from the 2011 breaklines, resulting in errors when comparing the elevation datasets. This made 2019 preprocessed DTM values higher in elevation than possible, which was further confirmed by processing a not hydro-flattened DTM, which cannot be used to compare the 2011 and 2019 elevation data. Parts of our study, particularly those involving DTM elevation and surface water level changes, relied on preprocessed data before identifying an error. If our partners replicate these methods, it could lead to hard-to-detect errors in their results. Consequently, we deem these specific methods unsuitable for our partners. Luckily, we recognized this error before we analyzed vegetation height, so our methods were different, relying on reprocessing the raw lidar point cloud. Although the error in the preprocessed data doesn't impact the methodology, it does require intricate lidar processing knowledge to reclassify the point cloud to create a digital surface model. Because of the potential difference in classification of ground vs. canopy points in both the 2011 and 2019 data, we believe the vegetation height change model is also not reliable for partner use.

We found that our classifications overestimated wetland extent compared to our partners' knowledge of wetland extent. Although the rest of our classification methods are feasible for partner use as it is a way to quantify wetland extent, manually creating training points was limited by the knowledge of the creator. Our training points were created in reference to available vegetation datasets, and it is likely that we created wetland points that were not actually wetlands on the ground. For example, if wetland training points covered both wetlands and sagebrush, the classification model would identify wetlands as covering a wider range of spectral signatures than they should. This can cause the classification to identify more areas as wetlands, such as sagebrush, than are present on the ground. The last limitation of our methods for partner use is that the 2060 classification is a model based on extrapolating data from two years and one predictor variable, not a definite rendition of the future. Because of this, it can be used as a reference to understand the general trend in wetland extent, but decisions should not be based solely on this product.

4.3 Future Recommendations

A few key implementations and changes emerged that will improve future application of the methods conducted in this study. Determining vegetation health, which is important to the partners for understanding where dead-standing cottonwood trees exist, and distinguishing vegetation type for classification could be improved with the inclusion of hyperspectral imagery. The classification modelling would also benefit from creating more accurate training sites with input from experts familiar with local wetland locations and incorporating field data for ground truthing. Incorporating field data would not necessarily require collecting new data, instead the field data collected during the creation of the Camas NWR Vegetation dataset could be used. Including high-resolution satellite imagery would also increase spatial precision, offering a better view of wetland dynamics and the ability to identify specific areas to target for conservation. Additionally, running the classification model for additional years, especially locally important water years such as during the 1980s, would provide a more holistic understanding of wetland change and trends. This would also help quantify historic restoration efforts by evaluating if there is a correlation between restoration and surface water extent. For TerrSet's Land Change Modeler, incorporating a broader array of environmental predictor variables, such as temperature and evapotranspiration, would help deepen insights into the factors influencing wetland conditions. Doing so would also make sure nuanced changes in climate, and its impact on wetlands, are captured by the model. Lastly, errors in the preprocessed data products from the lidar collected in 2019 must be rectified for ground elevation change to be analyzed with confidence that the changes shown are what happened on the land. This will most likely have to be done by reprocessing the raw lidar point cloud, or LAS data, to verify that the product being worked with is correct.

5. Conclusions

Our main purpose was to test the feasibility of using remote sensing to quantify wetland restoration efforts by determining wetland extent and change over time. To do this we used Landsat 8 imagery and manually created training sites as inputs in a Forest-based and Boosted Classification for 2016 and 2020, which resulted in output maps with greater than 84% validation accuracy. We then analyzed the differences and found that wetlands increased by 8%. Forecasting landcover to 2060, we found a predicted decrease in wetlands by 39% from 2020. Even though the findings from the ground elevation change and surface water change are not accurate due to errors in the preprocessed DTMs, we were able to accurately detect changes in vegetation height using lidar. Because we reprocessed the raw lidar point cloud from 2019 for the vegetation height change ourselves, the results were not impacted by the error in the preprocessed data. We found that the mean of +1.60 cm increase meant there was effectively no change in vegetation height across the entire study area. Upon visual inspection of smaller areas though, we did find some vegetation growth on the edges of riparian areas, with values up to 29.77 meters increase. We also visually found there to be decreases in vegetation height along riparian cottonwoods and willows, with decreasing vegetation height between 1 and 5 meters. The decline in vegetation height was expected but should also be validated with field data because some of the height change could be attributed to misclassification of canopy and ground points during lidar processing.

The results of our forecasted 2060 model indicate a notable decrease in wetland areas over the coming decades, signaling a need for partners to consider more restoration projects and water resource management and conservation strategies to address the predicted increase in temperature and decrease in precipitation. However, more analysis, including improving classifications and reprocessing the 2019 lidar data, will be needed before conclusions can be certain. Although the relatively limited knowledge of identifying the wetlands for remotely created classification points meant that the classification maps showed discrepancies compared to reality, our methodologies can help the USFWS and the IDFG with monitoring their wetlands, continuing to quantify new restoration projects, and making future decision-making supported by data. Additionally, our partners will be equipped to create new, tailored predictions to understand the current and possible future impacts of restoration work.

6. Acknowledgements

We would like to thank our Science advisor, Keith Weber, of ISU's GIS Training and Research Center, and our DEVELOP fellows, Jane Zugarek and Michael Pazmino for their guidance and support during this project. Additionally, we would like to acknowledge Ryan Healey for his contributions to developing the project's idea, and the staff and student interns at Idaho State University's GIS Training and Research Center for their encouragement and help.

We would also like to thank our partners from the U.S. Fish and Wildlife Service: Andrea Kristof, Brian Wehauer, Jeremy Timpey, & Michelle Campbell and our partners from the Idaho Department of Fish and Game: Brett Panting & Ailvie Freestorm.

Any opinions, findings, and conclusions or recommendations expressed in this material are those of the author(s) and do not necessarily reflect the views of the National Aeronautics and Space Administration.

This material is based upon work supported by NASA through contract 80LARC23FA024.

This material contains modified Copernicus Sentinel data (2016 - 2023), processed by ESA.

7. Glossary

Earth observations – Satellites and sensors that collect information about the Earth's physical, chemical, and biological systems over space and time.

Egin Bench – A farming area about 25 miles east of Mud Lake WMA. First settled in 1879, an old practice known as flood irrigation released huge amounts of water which returned to the watershed and filled the wetlands. A shift from flood irrigation to sprinkler irrigation in the Egin Bench area is theorized to have reduced surface and ground water in Mud Lake WMA in the 1990's.

Error of commission – The percentage of classification sites incorrectly identified as a certain class or were added to the specified classification class. This is calculated by adding together the incorrectly classified training sites (across the row) for a certain class and dividing them by the total number of validation sites for that class.

Error of omission – The percentage of classification sites identified incorrectly as other classes or left out of the specified classification class. This is calculated by adding together the incorrectly classified validation sites (down the column) for a certain class and dividing them by the total number of training sites for that class.

Flood irrigation – An ancient practice where large quantities of water are distributed over the field's surface to saturate the soil to water crops. Often it entails diverting streams and replenishing groundwater as a result.

GEE – Google Earth Engine which is linked to the USGS Earth Explorer and the European Space Agency Open Access Hub.

Ground water – Water that has infiltrated into the subsurface of Earth. May eventually replenish streams, rivers, and lakes.

Kappa, or Kappa coefficient – Evaluates the effectiveness or accuracy of a classification model compared to a classification in which the classes were randomly assigned to the classification sites. This value ranges from – 1 to 1, with the closer the value is to 1, the significantly better the classification model did than a random classification.

Palmer Severity Drought Index (PSDI) – A standardized index based on a simplified soil water balance, which estimates relative soil moisture conditions. It attempts to measure the duration and intensity of long-term drought. The Historical PSDI compares a PSDI for a certain period, say a month, to the 1901-2000 mean PSDI.

Producer's accuracy – The accuracy from the aspect of the map maker, usually meaning how often what is on the ground is correctly classified on the map. It is calculated by taking 100 and subtracting the error of

omission. It can also be calculated by taking the number correct on a column and dividing it by the total of sites along the same column.

Remote sensing – The acquiring of information from a distance, such as satellites which record reflected or emitted energy to provide data about processes on Earth.

Shallow flat – An area where the water is underground or very shallow for most of the year.

Sprinkler irrigation – A method of watering crops which mimics natural rainfall by spraying water from fixed or moving systems atop the land surface.

Surface reflectance – The fraction of incoming solar radiation that is reflected from Earth's surface to the Landsat sensor.

Surface water – Any body of water on Earth's surface, such as the ocean, streams, and lakes. More accessible than groundwater, making surface water important to humans and wildlife.

User's accuracy – The accuracy from the user's aspect usually means how often the class on the map is actually what is present on the ground. It is calculated by taking 100 and subtracting the error of commission. It can also be calculated by taking the number correct on a row and dividing it by the total of sites along the same row.

8. References

- Ashok, A., Rani, H. P., & Jayakumar, K. V. (2021). Monitoring of dynamic wetland changes using NDVI and NDWI based Landsat imagery. *Remote Sensing Applications: Society and Environment*, 23, 100547. <https://doi.org/10.1016/j.rsase.2021.100547>
- Banerjee, B. P., Raval, S., & Timms, W. (2016). Evaluation of rainfall and wetland water area variability at Thirlmere Lakes using Landsat time-series data. *International Journal of Environmental Science and Technology*, 13(7), 1781–1792. <https://doi.org/10.1007/s13762-016-1018-z>
- Camas National Wildlife Refuge. U.S. Fish & Wildlife Service. (n.d.). Retrieved February 13, 2024, from <https://www.fws.gov/refuge/camas>
- Copernicus Sentinel-2. (n.d.). S2 Mission - Acquisition Resolutions. *Copernicus Sentinel-2 User Guides*. Retrieved March 21, 2024, from <https://sentiwiki.copernicus.eu/web/s2-mission#S2-Mission-Acquisition-Resolutions>
- Dahl, T.E. (1990). *Wetland Losses in the United States 1780's to 1980's*. U.S. Department of the Interior, Fish and Wildlife Service. <https://www.fws.gov/sites/default/files/documents/Wetlands-Losses-in-the-United-States-1780s-to-1980s.pdf>
- European Space Agency. (ESA). (2016). *Sentinel-2 MSI: Multispectral Instrument* [Dataset]. Earth Engine Data Catalog/USGS. https://doi.org/10.5270/S2_-6eb6imz
- Herndon, K., Muench, R., Cherrington, E., & Griffin, R. (2020). An Assessment of Surface Water Detection Methods for Water Resource Management in the Nigerien Sahel. *Sensors*, 20(2), 431. <https://doi.org/10.3390/s20020431>
- Hogan, R. (2006). How to combine errors. University of Reading, Meteorology Department https://www.met.rdg.ac.uk/~swrhgnrj/combining_errors.pdf
- Huang, C., Peng, Y., Lang, M., Yeo, I., & McCarty, G. (2014) Wetland inundation mapping and change monitoring using Landsat and airborne LiDAR data. *Remote Sensing of Environment*, 141, 231-242. <https://doi.org/10.1016/j.rse.2013.10.020>.

- LANDFIRE. (2022). Us_230 Existing Vegetation Type. [Data set]. LANDFIRE. Retrieved March 05, 2023. <https://www.landfire.gov/viewer/>
- Ma, F., Wang, Q., & Zhang, M. (2018). Dynamic changes of wetland resources based on MODIS and Landsat image data fusion. *EURASIP Journal on Image and Video Processing*, 2018(1), 63. <https://doi.org/10.1186/s13640-018-0305-7>
- Mud Lake WMA*. Idaho Fish and Game. (2023). Retrieved February 12, 2024, from <https://idfg.idaho.gov/visit/wma/mud-lake>
- Naik, B.C., & Anuradha, P.B. (2018). Water Body Extraction Using Images From Two Different Satellites Over Chilika Lake. *International Journal of Electronics Engineering*, 10(1) 140-145. <https://www.csjournals.com/IJEE/PDF10-1/29.%20CN.pdf>
- NAIP National Agriculture Imagery Program. (2021). [Data Set]. NAIP National Agriculture Imagery Program. Retrieved March 11, 2024. <https://gis.apfo.usda.gov/arcgis/rest/services/NAIP>
- NOAA National Centers for Environmental Information. (2024). Climate at a Glance: Divisional Rankings. [Data Set]. NOAA National Centers for Environmental Information. Retrieved February 07, 2024. <https://www.ncei.noaa.gov/access/monitoring/climate-at-a-glance/divisional/rankings>
- Ozesmi, S. L., & Bauer, M. E. (2002). Satellite remote sensing of wetlands. *Wetlands Ecology and Management*, 2002, 10, 381-402. <https://doi.org/10.1023/A:1020908432489>
- Sharma, S. K., & Anjaneyulu, D. (1993). Application of remote sensing and GIS in water resource management. *International Journal of Remote Sensing*, 14(17), 3209-3220. <https://doi.org/10.1080/01431169308904435>
- U.S. Fish and Wildlife Service. (2012). *Camas National Wildlife Refuge Vegetation Inventory, Classification, and Mapping*. [Data Set]. Andrea Kristof. <https://ecos.fws.gov/ServCat/DownloadFile/40667?Reference=40925>
- U.S. Fish and Wildlife Service. (2014). *Camas National Wildlife Refuge Draft Comprehensive Plan and Environmental Assessment*. [Unpublished manuscript].
- U.S. Geological Survey Earth Resources Observation and Science Center. (2020). *Landsat 5 TM* [Data set]. US Geology Survey. <https://www.usgs.gov/centers/eros/science/usgs-eros-archive-landsat-archives-landsat-4-5-thematic-mapper-collection-2>
- U.S. Geological Survey Earth Observation and Science Center. (2020). *Landsat 8 OLI/TIRS* [Data set]. US Geological Survey. <https://www.usgs.gov/centers/eros/science/usgs-eros-archive-landsat-archives-landsat-8-9-operational-land-imager-and>
- U.S. Geological Survey. (2023). *ID Southern ID_2018_D19 WUID: 300188* [Data set]. Dewberry Engineers Inc. https://app.globus.org/file-manager?origin_id=03bed01a-e124-11e7-802a-0a208f818180&origin_path=%2Fprocessed%2FEastern%2FSouthernIdaho2018_14%2F
- Watershed Sciences, Inc. (2012). *LiDAR Remote Sensing Data Collection: Camas National Wildlife Refuge, Idaho* [Data set]. Watershed Sciences, Inc. [Camas National Wildlife Refuge – Idaho Lidar Consortium](https://www.watershedsciences.com/Camas-National-Wildlife-Refuge-Idaho-Lidar-Consortium)

9. Appendices

Appendix A (Tables)

Table A1.

Revised Transition Probability Matrix for 2060 Land Change Modeler. This table shows the probability of one class transitioning to another class between 2020 and 2060. For example, USWFS and IDFG will not be expanding any roads or buildings, nor will they be converting any more areas to crops, so both the developed and crops classes have values of 1, indicating that they will not change.

	Water	Wetland	Developed	Sagebrush	Crops
Water	0.9833	0.0165	0.0000	0.0002	0.0000
Wetland	0.1520	0.7050	0.0000	0.1430	0.0000
Developed	0.0000	0.0000	1.0000	0.0000	0.0000
Sagebrush	0.0009	0.0124	0.0000	0.9867	0.0000
Crops	0.0000	0.0000	0.0000	0.0000	1.0000

Table A2.

Confusion Matrix 2016. This confusion matrix was made for our 2016 Forest-based and Boosted Classification by comparing the results from the training sites to the results from the validation sites. The overall accuracy was 86.52%, and the Kappa value was 0.83, indicating our classification did significantly better than a random classification.

Class	1	2	3	4	5	Total	User's Accuracy
1	40	0	0	0	0	40	100%
2	1	70	7	3	0	81	86.42%
3	1	3	40	3	4	51	78.43%
4	1	2	7	48	1	59	81.36%
5	1	0	0	1	33	35	94.29%
Total	44	75	54	55	38	266	
Producer's Accuracy	90.90%	93.33%	74.07%	85.71%	86.84%		86.52%

Table A3.

Confusion Matrix 2020. This confusion matrix was made for our 2020 Forest-based and Boosted Classification by comparing the results from the training sites to the results from the validation sites. The overall accuracy was 84.27%, and the Kappa value was 0.80, indicating our classification did significantly better than a random classification.

Class	1	2	3	4	5	Total	User's Accuracy
1	42	1	1	0	1	45	93.33%
2	2	64	3	10	1	80	80.00%
3	0	7	46	3	5	61	75.41%
4	0	2	4	42	0	48	87.50%
5	0	1	0	0	31	32	96.88%
Total	44	75	54	56	38	266	
Producer's Accuracy	95.45%	85.33%	85.19%	75.00%	81.58%		84.27%

Appendix B (Equations)

$$NDVI = Index (NIR, RED) = \frac{NIR - RED}{NIR + RED} \quad (\text{Eq. B1})$$

Equation B1. Normalized Difference Vegetation Index (NDVI) *NIR* refers to Near Infrared band value (Band 5, 0.85–0.88 μm) and *RED* refers to the visible red band value (Band 4, 0.64–0.67 μm) for NASA’s Landsat 8 OLI sensor (Herndon et al., 2020). For Sentinel-2, NIR is Band 8 (0.84 μm), and RED is Band 4 (0.67 μm) (Copernicus Sentinel-2, n.d.).

$$MNDWI = Index (GREEN, SWIR) = \frac{GREEN - SWIR}{GREEN + SWIR} \quad (\text{Eq. B2})$$

Equation B2. Modified Normalized Difference Water Index (MNDWI) equation where Green is the visible green band value (Band 4, 0.53–0.59 μm) and *SWIR* refers to Near Infrared band value (Band 6, 1.57–1.65 μm) for NASA’s Landsat 8 OLI sensor (Herndon et al., 2020).

$$\text{combined root mean square error} = \sqrt{(\text{error}_1)^2 + (\text{error}_2)^2} \quad (\text{Eq. B3})$$

Equation B3. The combined error covariance equation integrates vertical error values from different temporal datasets in lidar measurements, offering a comprehensive understanding of the overall uncertainty in elevation data over time between 2011 and 2019 (Hogan, 2006).

Appendix C (Charts)

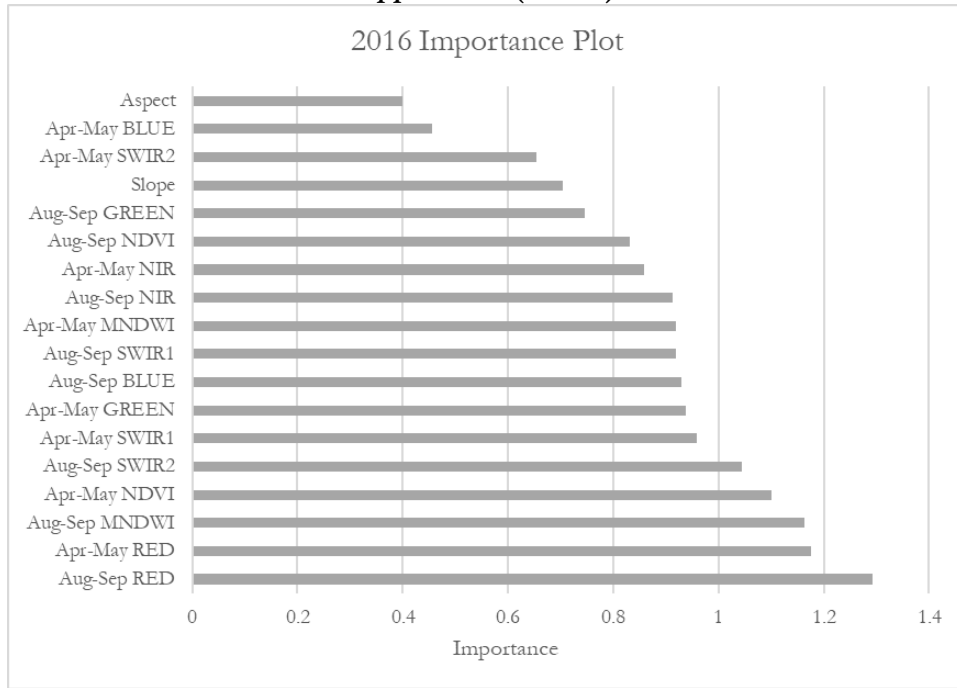


Figure C1. Importance plot 2016. This chart shows the value of importance for each variable for the Forest-based and Boosted Classification for 2016. The higher the value, the more important the variable was, meaning the model used it more to make decisions between different classes for each pixel.

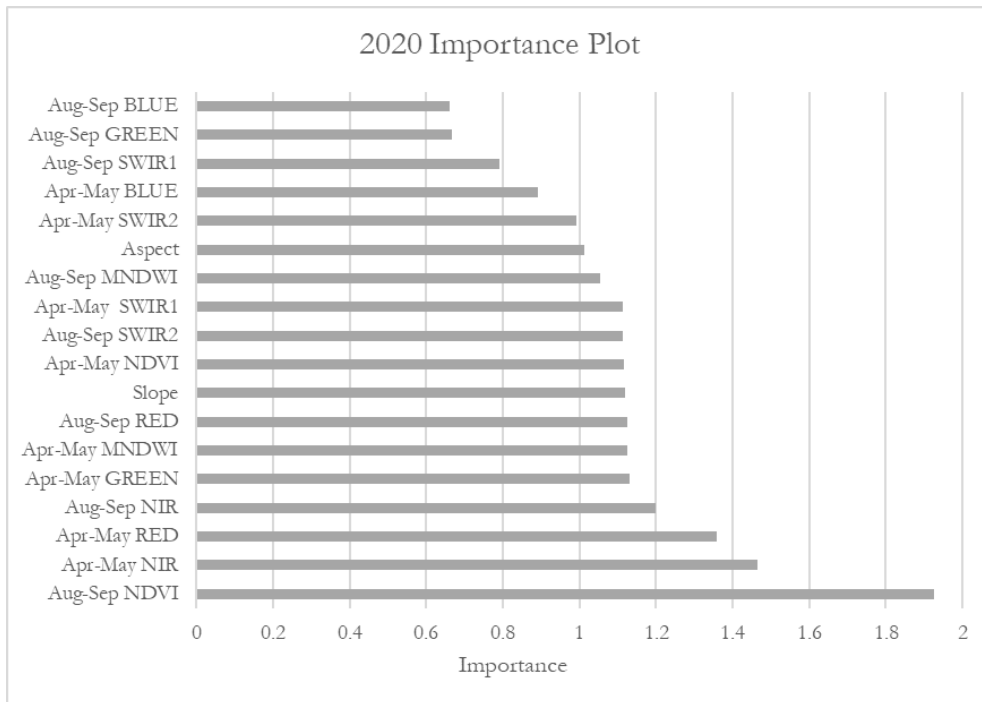


Figure C2. Importance plot 2020. This chart shows the value of importance for each variable for the Forest-based and Boosted Classification for 2020. The higher the value, the more important the variable was, meaning the model used it more to make decisions between different classes for each pixel.

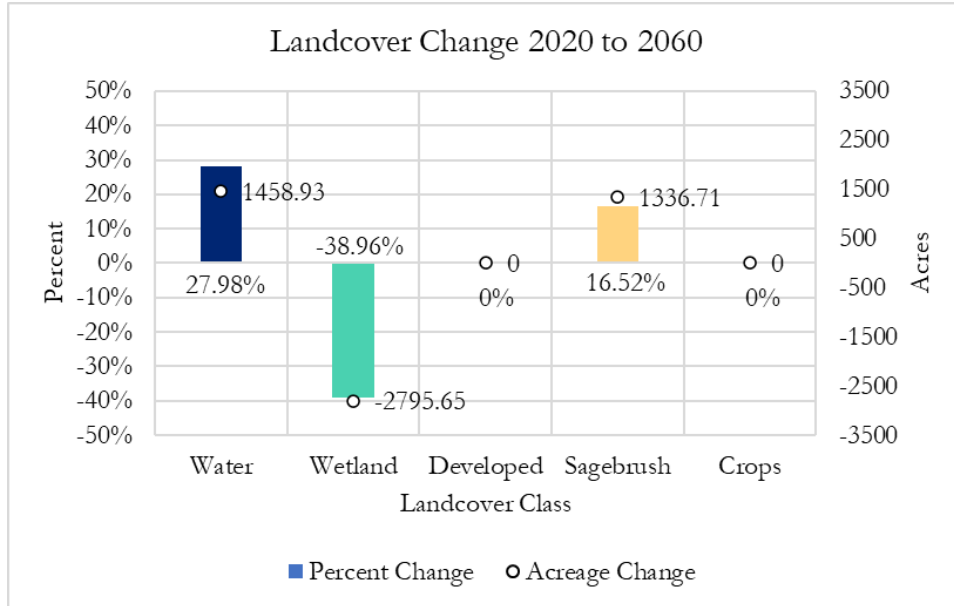


Figure C3. Changes between 2020 and 2060 in landcover classes. This chart shows the differences, in percentage and acreage for each of our 5 landcover classes, between our 2020 classification model and our 2060 predicted model. Each landcover class is identified by name and with the corresponding color used for it on the 2020 and 2060 maps.

Appendix D (Figures)

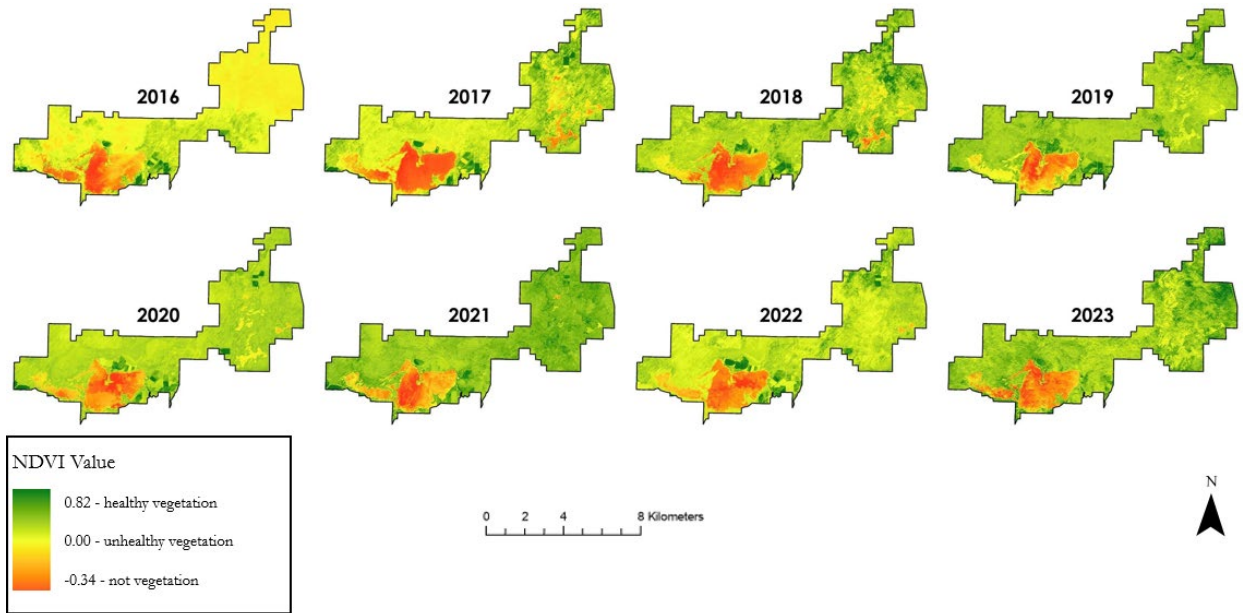


Figure D1. NDVI time series derived from Sentinel-2 data. Values close to one, which are dark green on the maps, represent healthy vegetation. Values closer to zero, or yellow, show unhealthy vegetation such as dry grass and stressed herbaceous plants. Values close to zero are non-vegetation features such as water.

Figure D2A

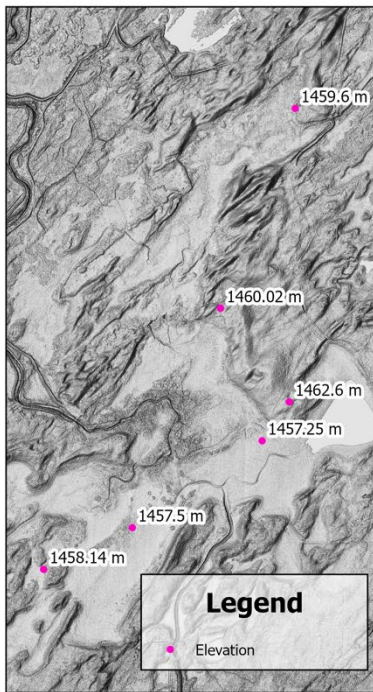


Figure D2B

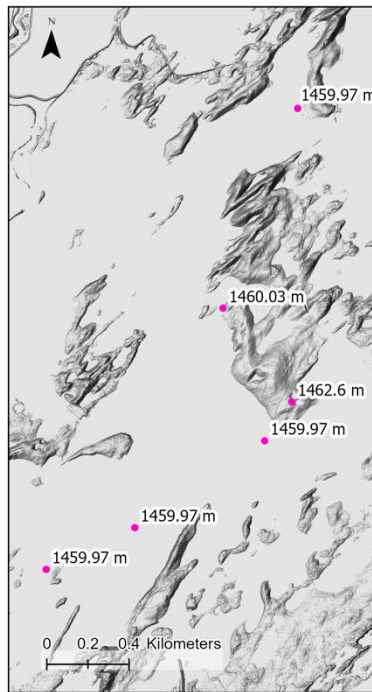


Figure D2C

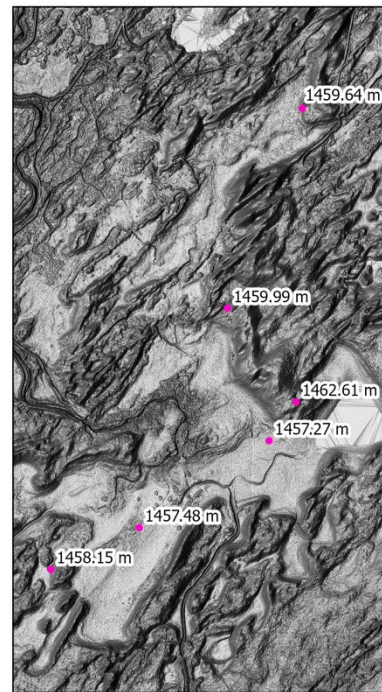


Figure D2. Figure D2A displays the ILC's hydro-flattened DTM for 2011, while Figure D2B presents the 2019 hydro-flattened DTM product, also an ILC product. Figure D2C showcases a 2019 DTM derived from raw lidar data without hydro-flattening, produced from raw lidar data provided by the ILC. All figures focus on Ray's Lake, positioned centrally at the bottom, within a region of flat-appearing topography. The comparison

highlights discrepancies in elevation across the figures: notably, Figure D2B's elevations vary up to one to two meters in the flat areas near the bottom of the map, especially near Ray's Lake, compared to both the 2011 hydro-flattened product (Figure D2A) and the 2019 un-hydro-flattened DTM (Figure D2C), pinpointing discrepancies in the 2019 hydro-flattened product to the 2011 hydro-flattened data. The un-hydro-flattened state of Figure D2C precludes its use for direct elevation difference calculations between 2019 and 2011.

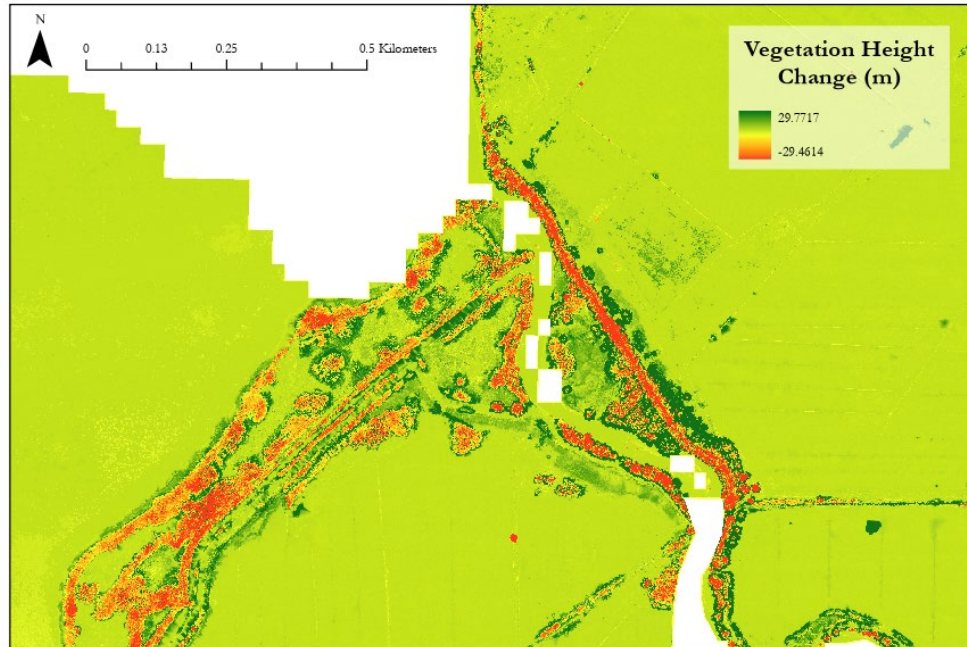


Figure D3. Vegetation Height Change Map for a southeast corner of Mud Lake WMA. This map was derived from lidar data and was created by subtracting the Digital Surface Model (DSM) for 2011 from the Digital Surface Model for 2019 to show change between the two years. The dark green shade represents where there was new vegetation in 2019, or where it grew taller from 2011. The red shade represents where the vegetation was shorter in 2019 than 2011.

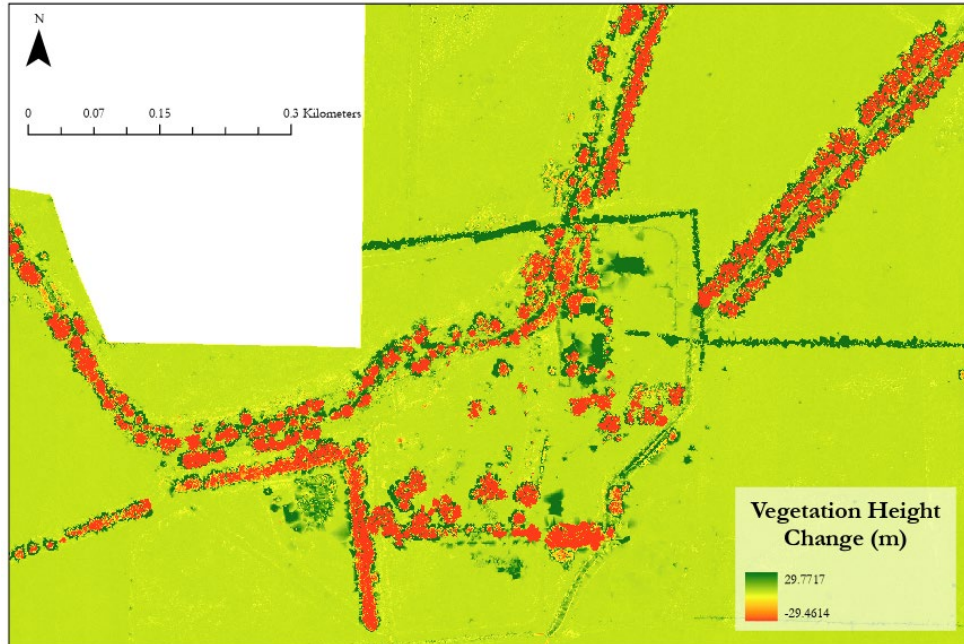


Figure D4. Vegetation Height Change Map for a northern part of Camas NWR highlighting the planted Shelter Belt cottonwood trees. This map was derived from lidar data and was created by subtracting the Digital Surface Model (DSM) for 2011 from the Digital Surface Model for 2019 to show change between the two years. The dark green shade represents where there was new vegetation in 2019, or where it grew taller from 2011. The red shade represents where the vegetation was shorter in 2019 than 2011.

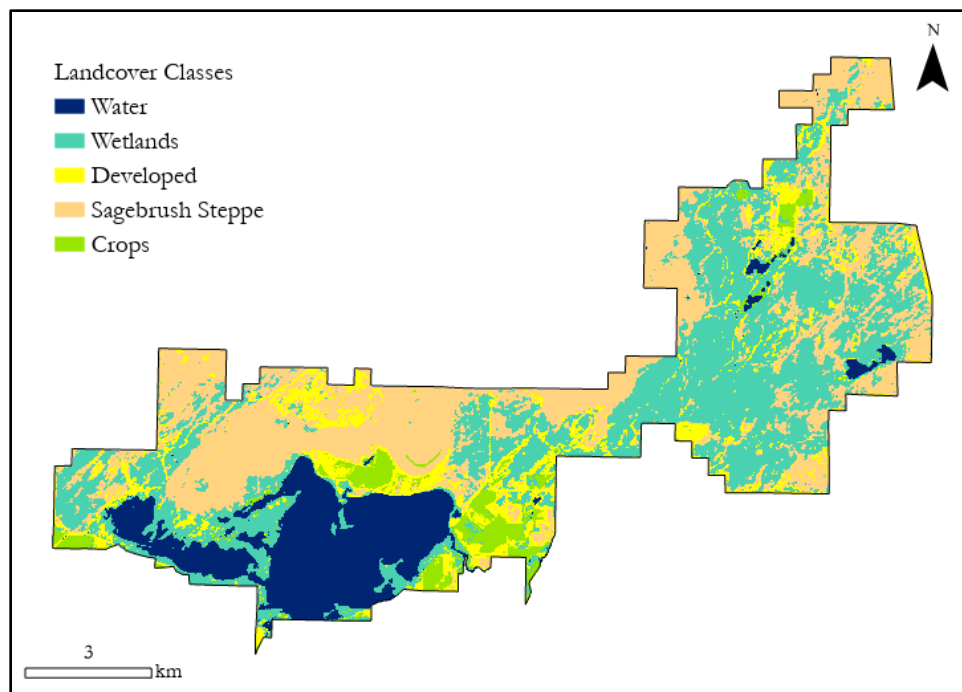


Figure D5. Forest-based and Boosted Classification map from 2016 for Mud Lake WMA and Camas NWR.

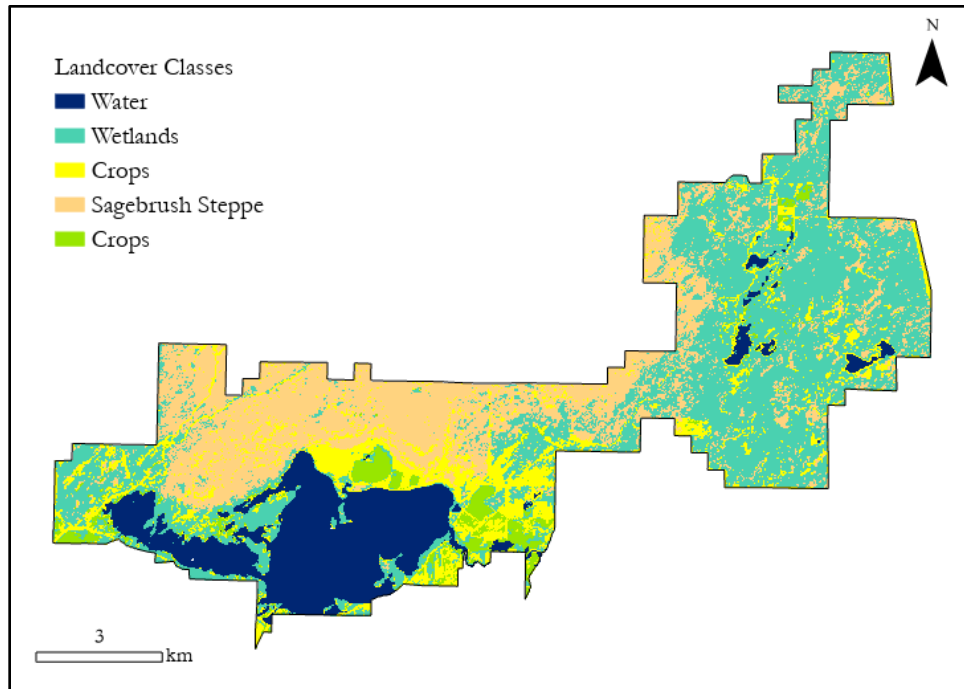


Figure D6. Forest-based and Boosted Classification map from 2020 for Mud Lake WMA and Camas NWR.

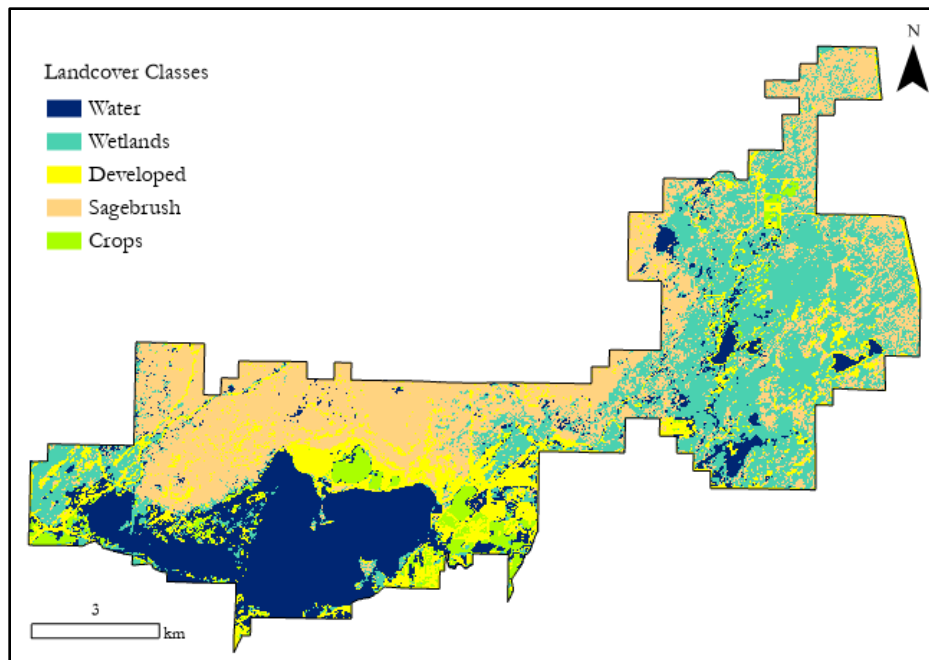


Figure D7. Forecasted classification map for 2060 created using TerrSet Land Change Modeler over Mud Lake WMA and Camas NWR.